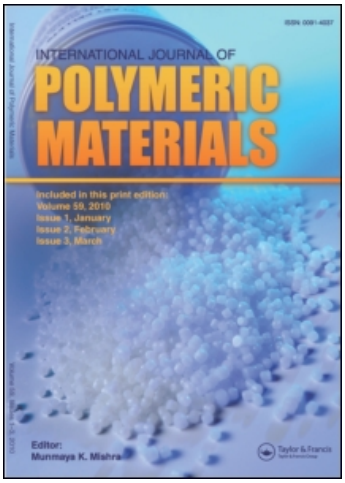

International Journal of Polymeric Materials
Publication details, including instructions for authors and subscription information:
http://www.informaworld.com/smpp/title~content=t713647664

Viscoelasticity of Polydisperse Polymers at the Extensional Flow

I. P. Briedis[a]; V. V. Leitland[a]
[a] Institute of Polymer Mechanics, Latvian SSR Academy of Sciences, Riga, U.S.S.R.

To cite this Article Briedis, I. P. and Leitland, V. V.(1982) 'Viscoelasticity of Polydisperse Polymers at the Extensional Flow', International Journal of Polymeric Materials, 9: 3, 167 — 186
To link to this Article: DOI: 10.1080/00914038208077978
URL: http://dx.doi.org/10.1080/00914038208077978

Intern. J. Polymeric Mater., 1982, Vol. 9, pp. 167–186
0091–4037/82/0903–0167 $06.50/0

Printed in Great Britain

Viscoelasticity of Polydisperse Polymers at the Extensional Flow†

I. P. BRIEDIS and V. V. LEITLAND

Institute of Polymer Mechanics, Latvian SSR Academy of Sciences, Riga, 226006, U.S.S.R.

(*Received June 4, 1981*)

Pre-stationary elongational flow of polymers is investigated. Viscoelastic properties of stretched test samples are determined with linear periodic deformation superimposed on elongational flow. A generalized Maxwell model is used to describe viscoelastic properties; a model based on frequency relation averaging for dynamic viscosities of monodisperse fractions forming a polydisperse polymer is suggested to define a relationship between viscoelastic characteristics and molecular parameters of a test sample. It is shown that the deformation response of a fluid polymer under stretching becomes similar to that of a solid body.

The advent of polymeric materials urged rejection of conventional theories under which shear flow was used to study the properties of fluids, while those of elastic and plastic solid bodies were investigated under uniaxial extension conditions. In recent years, a number of test devices have been designed to be used in studying uniaxial extension of polymeric fluids. Considerable efforts have been directed towards theoretical developments enabling a polymer melt or solution to be determined for its uniaxial extension resistance based on the shear deformation results. Previous studies have shown the molecular weight distribution (MWD) width to have an exclusively high effect with respect to the elongational flow resistance *vs.* kinematic flow characteristics relationship. Extension of narrow molecular weight distribution (NMWD) polymer fluids always leads either to a steady flow condition at low strain rates, or to a test sample breakage before steady flow conditions are attained at high strain rates.[1,3] In any case, monodisperse polymers flow under constant viscosity conditions. As it has been noted in most cases for a number of polydisperse polymers, elongational viscosity increases with strain rate, with an extra-

† Presented at the XI All-Union Symposium on Polymer Rheology, March 12–16, 1980, Suzdal (U.S.S.R.).

ordinarily long pre-stationary flow region being observed. Without going into details of the well-known experimental results reviewed in[4,5] it should be noted that no systematic studies of molecular structure effects on elongational flow of polydisperse materials have been undertaken.

Our studies of the polyisobutylene behavior under stationary flow conditions at high strain rates (as compared with the characteristic relaxation time)† have shown that the material exhibits no pre-stationary flow termination symptoms with the test sample elongated up to 50 times its original length. Only with stretching degree reaching 50 to 150 times the original sample length, there occurs a comparatively sharp transition of the stress to a constant value (Figure 1) at a constant elongational strain rate. The

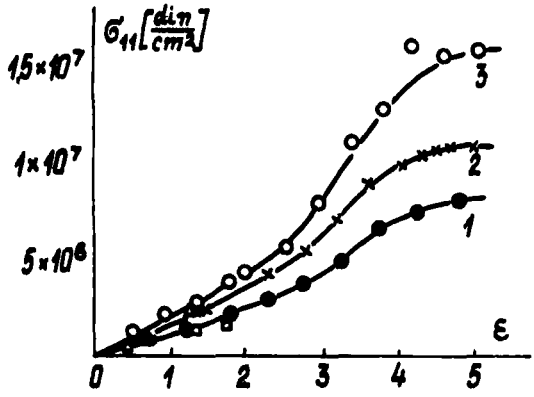

FIGURE 1 Stress σ_{11} *vs.* strain relationship for polyisobutylene PiB-20 at 19°C. Strain rate $\dot{\varepsilon}$, sec^{-1}: 1, 0.043; 2, 0.071; 3, 0.1.

elongational strain value at which steady elongational flows are attained increases with the strain rate. Similar results were obtained in[6] for low-density polyethylene. The results in Figure 1 have been acquired under special conditions using a Meissner-type apparatus as described elsewhere.[7]

The pre-stationary flow takes place at stretching degrees of practical significance (Figure 2).

When comparing the niaxial extension results for the polyethylene melt with the calculations using five models, it may be seen that the best results are obtained for the generalized Maxwell model.[8] For this model expressed as

$$\sigma^{ij} + \tau D\sigma^{ij}/Dt = 2\eta\dot{\varepsilon}^{ij} \tag{1}$$

† The term "characteristic relaxation time" should be understood as an inverse value of the frequency at which the peak in a frequency relaxation spectrum occurs.

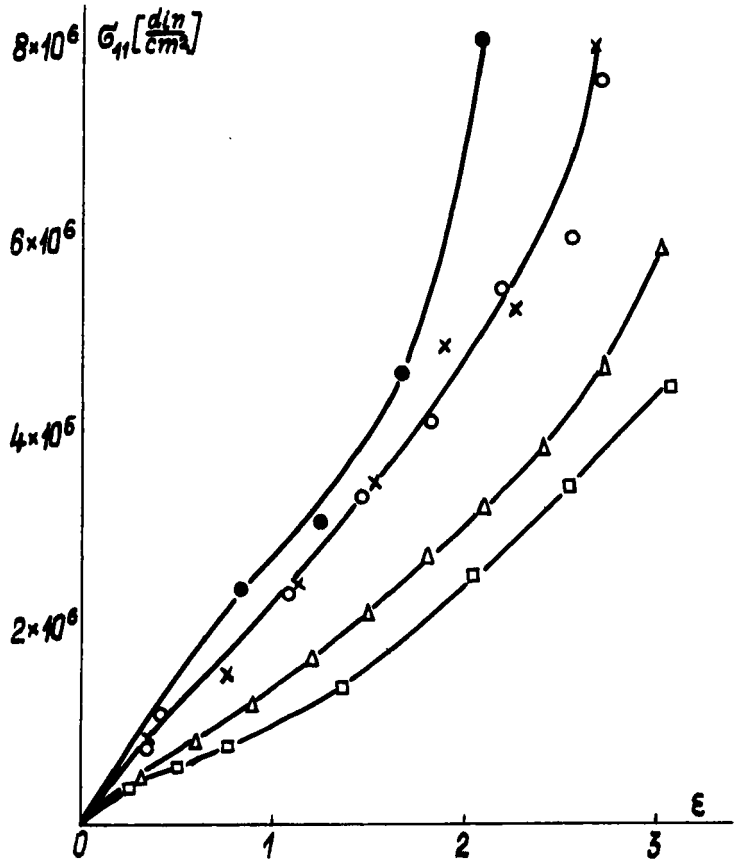

FIGURE 2 Stress *vs.* strain relationship for polyisobutylene PiB-20 at 19°C. Strain rate $\dot{\varepsilon}$, sec^{-1}: □, 0.0427; △, 0.05; ×, 0.122; ○, 0.126; ●, 0.14.

the converted derivative by Oldroyd

$$\frac{D\sigma^{ij}}{Dt} = \frac{\partial \sigma^{ij}}{\partial t} + V^k \frac{\partial \sigma^{ij}}{\partial X_k} - \frac{\partial V^i}{\partial X_k}\sigma^{kj} - \frac{\partial V^j}{\partial X_k}\sigma^{ik}$$

will be taken, where V^k is the velocity vector component. In Eq. (2), g^{ik} are the metric tensor components, and the strain rate is given by

$$\dot{\varepsilon}^{ij} = \frac{1}{2}\left(\frac{\partial V^i}{\partial X_k} g^{ik} + \frac{\partial V^i}{\partial X_k} g^{kj}\right) \tag{2}$$

The continuity equation will be written in cylindrical coordinates:

$$\frac{1}{R}\frac{\partial}{\partial R} R V_R + \frac{1}{R}\frac{\partial V_\theta}{\partial \theta} + \frac{\partial V_z}{\partial z} = 0 \tag{3}$$

Consideration will be given to the deformation conditions with the sample length being much smaller than the elongational strain wavelength in the material. In this case, V_z is independent of the elongation coordinate. With these assumptions in view, Eq. (1) solutions for the deformation conditions

$$\frac{dV_z}{dz} = \dot{\varepsilon} = \text{const} \tag{4}$$

$$\frac{dV_z}{dz} = \dot{\varepsilon} + \varepsilon_0 \omega \cos \omega t \tag{5}$$

are known and, upon generalization to infinite number of the Maxwell elements, acquire the following form:

a) under stationary flow conditions

$$\sigma_{11} = \dot{\varepsilon} \int_0^\infty 2\left(\frac{1-e^{-(S-2\dot{\varepsilon})t}}{S-2\dot{\varepsilon}} + \frac{1-e^{-(S+\dot{\varepsilon})t}}{S+\dot{\varepsilon}}\right) N(S)\, dS \tag{6}$$

where $S = 1/\tau$ is the relaxation frequency;

b) with periodic deformation superimposed on the stationary flow, the solution obtained may be used to determine the complex elongational modulus components E' and E'' as the periodic stress component to periodic strain component ratios:

$$E' = \int_0^\infty \left\{2\frac{\omega^2 - 2\dot{\varepsilon}(S-2\dot{\varepsilon})}{(S-2\dot{\varepsilon})^2+\omega^2} + \frac{\omega^2 + \dot{\varepsilon}(S+\dot{\varepsilon})}{(S+\dot{\varepsilon})^2+\omega^2} + \dot{\varepsilon}\left[4\frac{1-e^{-(S-2\dot{\varepsilon})t}}{S-2\dot{\varepsilon}} - \frac{1-e^{-(S+\dot{\varepsilon})t}}{S+\dot{\varepsilon}}\right]\right\} N(S)\, dS \tag{7}$$

$$E'' = \omega \int_0^\infty S\left[\frac{2}{(S-2\dot{\varepsilon})^2+\omega^2} - \frac{1}{(S+\omega)^2+\omega^2}\right] N(S)\, dS \tag{8}$$

The molecular structure effect on the elongational flow characteristics is expressed using the relaxation spectrum $N(S)$. For this relation to be established, the viscosity summation concept suggested in Ref. 3 will be used. For a polydisperse polymer having a long-chain branching of molecules, the initial viscosity of the melt will be represented as function of molecular parameters:

$$\eta_0 = k(\bar{M}_w \langle g \rangle_w f(u))^\theta \tag{9}$$

where

$\langle g \rangle_w$ = weight-average conformation coefficient value for a branched molecule;

$f(u)$ = Schulz polydispersity index function;

k, θ = constants;

$\bar{M}_w$ = weight-average molecular weight given by

$$\bar{M}_w = \int_0^\infty MW(M)\, dM \tag{10}$$

with $\int_0^\infty W(M)\, dM = I$. Substitution of Eq. (10) into Eq. (9) yields

$$\eta_0 = k\left\{\langle g\rangle_w f(u) \int_0^\infty MW(M)\, dM\right\}^\theta \tag{11}$$

Let us represent the polydisperse polymer as a blend of close-cut fractions for which the following ratio holds true:

$$\eta_{0f} = k(gM)^\theta \tag{12}$$

As follows, e.g. from Ref. 9, constant k and θ in Eqs. (9) and (12) are the same. Then, representing the Eq. (11) molecular fraction weight M in terms of a respective initial viscosity gives

$$\eta_0 = \left\{\langle g\rangle_w f(u) \int_0^\infty g^{-1}\eta_{0f}^{1/\theta}\, W(M)\, dM\right\}^\theta \tag{13}$$

Generalizing summation rule Eq. (13) to the frequency relation of the dynamic viscosity yields

$$\eta'(\omega) = \left\{\langle g\rangle_w f(u) \int_0^\infty g^{-1}[\eta'_f(k_\tau, \omega)]^{1/\theta}\, W(M)\, dM\right\}^\theta \tag{14}$$

This generalization introduces a coefficient (k_τ) into the expression of each frequency relation of the fraction viscosity, k_τ being the relaxation time-shift coefficient for the fraction in a mixture with other fractions.[10,11]

The frequency relation $\eta'_f(k_\tau, \omega)$ of an elementary fraction will be specified in the following form:

$$\eta'_f = \frac{\eta_{0f}}{1 + (k_\tau \omega\tau)^{\alpha_0}} \tag{15}$$

As follows from Ref. 12, the relaxation time-shift coefficient of the fraction in a mixture with other fractions is expressed in terms of molecular characteristics and initial viscosity:

$$k_\tau = M\eta_0/\bar{M}_w\eta_{0f} \tag{16}$$

Using Eqs. (9) and (12), the viscosities will be represented in terms of molecular

parameters:

$$k_\tau = \left(\frac{\bar{M}_w}{M}\right)^{\theta-1}\left(\frac{\langle g\rangle_w}{g}\right)^{\theta} f^{\theta}(u) \tag{17}$$

It is suggested in Ref. 12 that the $\bar{M}_w/M$ ratio power may differ from $\theta-1$ and therefore should be determined experimentally. Hence, k_τ will be written in the following form:

$$k_\tau = \left(\frac{\bar{M}_w}{M}\right)^{\beta}\left(\frac{\langle g\rangle_w}{g}\right)^{\beta+1} f^{\beta+1}(u) \tag{18}$$

Normally, the characteristic relaxation time for monodisperse polymers is considered to be a function of molecular parameters, similarly to the initial viscosity:

$$\tau = k_\tau(gM)^{\theta} \tag{19}$$

Equations (12), (18) and (19) enable the frequency relation of the elementary fraction from Eq. (15) to be determined according to appropriate molecular parameters:

$$\eta'_f = \frac{k(gM)^{\theta}}{1+[\omega\langle g\rangle_w^{\beta+1}\bar{M}_w^{\beta}g^{\theta-\beta-1}M^{\theta-\beta}f^{\beta+1}(u)]^{\alpha_0}} \tag{20}$$

In order to use Eq. (20), the long-chain branching characteristic (g) be expressed as a function of the molecular weight.

The number of long-chain branches may be accounted for by using the Mendelson–Drott hypothesis,[13] under which the long-chain branching node number (n) is proportional to the molecular weight of a fraction:

$$n = lM \tag{21}$$

To define the relationship between the long-chain branching node number and the conformation coefficient (g), the well-known Zimm–Stockmayer relation[14,15] will be used:

$$g = \left(\sqrt{\sqrt{1-lM/7} - \frac{4lM}{9\pi}}\right)^{-1} \tag{22}$$

Equation (14) together with Eqs. (20) and (22) enables the frequency relation of the dynamic viscosity to be computed on the basis of molecular parameters $\bar{M}_w$, u, $\langle g\rangle_w$.

Since $G'' = \omega\eta'$, the frequency relaxation spectrum may be calculated from Eq. (14). To do this, the following equation from Ref. 16 may be used:

$$N(S) = \frac{2}{\pi S}\,\mathrm{Re}\; G''(Se^{\pm i(\pi/2)}) \tag{23}$$

Then, the following expression is obtained from Eq. (14) for the spectrum:

$$N(S) = \frac{2}{\pi S}\left\{\langle g\rangle_w f(u)\int_0^\infty \mathrm{Re}[Se^{\pm i(\pi/2)}(\eta'(Se^{\pm i(\pi/2)}))^{1/\theta} g^{-1} W(M)\, dM]\right\}^\theta \quad (24)$$

For practical applications, an approximated calculation method seems to be more convenient. Here, the dynamic viscosity of a polydisperse polymer is approximated by means of the following equation:†

$$\eta' = \frac{\eta_0}{1+(\omega\tau_r)^\alpha} \quad (25)$$

As shown in Refs. 17 and 18, Eq. (25) provides rather a good description for viscoelastic properties of a polymer melt. If Eq. (14) is taken equal to Eq. (25) with Eq. (14) representing viscosity in terms of molecular parameters from Eq. (20), then an equation is obtained to be used for calculations of the characteristic relaxation time at frequency $\omega = I/\tau_r$:

$$\frac{2}{\bar{M}_w}\int_0^\infty \frac{MW(M)\, dM}{\{1+[k_1\tau_r^{-1}\langle g\rangle_w^{\beta+1}\bar{M}_w^\beta g^{\theta-\beta-1}M^{\theta-\beta}f^{\beta+1}(u)]^{\alpha_0}\}^{1/\theta}} - 1 = 0 \quad (26)$$

Once the characteristic relaxation time is known, a relation may be defined at frequency $\omega = m_t/\tau_r$ to be used for determination of the dynamic viscosity reduction rate factor:

$$\alpha = \frac{1}{\log m_t}\log\left\{\frac{\bar{M}_w^\theta}{\left\{\int_0^\infty \frac{MW(M)\, dM}{[1+(m_t/\tau_r\langle g\rangle_w^{\beta-1}\bar{M}_w^\beta M^{\theta-\beta}g^{\theta-\beta-1}f^{\beta+1}(u))^{\alpha_0}]^{1/\theta}}\right\}^\theta} - 1\right\} \quad (27)$$

According to Eq. (23), the dynamic viscosity determined by Eq. (25) has a corresponding frequency relaxation spectrum:

$$N(S) = \frac{2}{\pi}\eta_0 \sin\frac{\alpha\pi}{2}\frac{(\tau_r S)^\alpha}{1+2(\tau_r S)^\alpha\cos\dfrac{\alpha\pi}{2}+(\tau_r S)^{2\alpha}} \quad (28)$$

The relaxation spectrum from Eq. (28) is specified with three constants which may be calculated from Eqs. (9), (26), (27) on the basis of molecular parameters. Subsequently, Eq. (6) may be used to investigate the molecular structure effect on the stationary elongational flow development and, in conjunctions with Eqs. (7) and (8), to determine the molecular structure effect on viscoelasticity characteristics.

† The use of approximation Eq. (25) is in no way mandatory; other analytical equations may be used to describe the relation as well.

Figure 3 shows the stress *vs.* strain relationship for the uniaxial stress state calculated using Eq. (6). The calculations are made for the log normal MWDs with several weight-average values. When at the same strain rate, low MW samples rapidly reach the steady elongational flow conditions. In the cases of higher MW values, the stress increases with extension; the higher the MW, the quicker the increase. Such an effect of the MW is enhanced with increasing strain rates.

Quite unique is the MWD width effect on the elongitudinal flow development. The MWD width affects the viscous properties of a polymer to rather a small extent, whereas the relaxation time is much more sensitive to changes in molecular weight polydispersity. Changing the MWD width offsets the $N(S)$

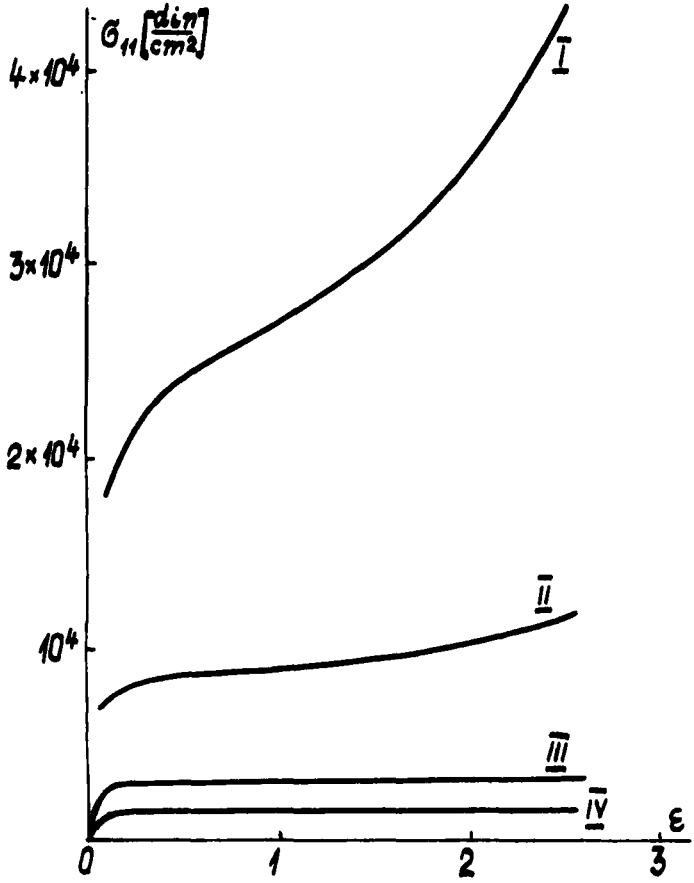

FIGURE 3 Weight-average molecular weight effect on the stress *vs.* strain relationship under pre-stationary elongational flow conditions at strain rate $\dot{\varepsilon} = 0.00137$. $\bar{M}_w$: I, $3.65 \cdot 10^5$; II, $2.74 \cdot 10^5$; III, $2 \cdot 10^5$; IV, $1.641 \cdot 10^5$.

spectrum peak, therefore the characteristic relaxation time increases with the MWD width. Two $\sigma - \varepsilon$ curves for a BMWD sample and a NMWD sample at the same strain rate may be distinguished in that, at the beginning (at low ε's), the BMWD curve is located below the NMWD curve. The strain development process reverses the two curve locations: the stress in the BMWD sample becomes higher than that in the NMWD sample. The above MWD effect on the stationary flow development is more pronounced at higher strain rates (Figure 4).

Increasing the molecular branching affects the initial $\sigma - \varepsilon$ relation stage in the manner similar to that of decreasing molecular weights. This is a qualitative similarity only, since the manner the viscosity and the charac-

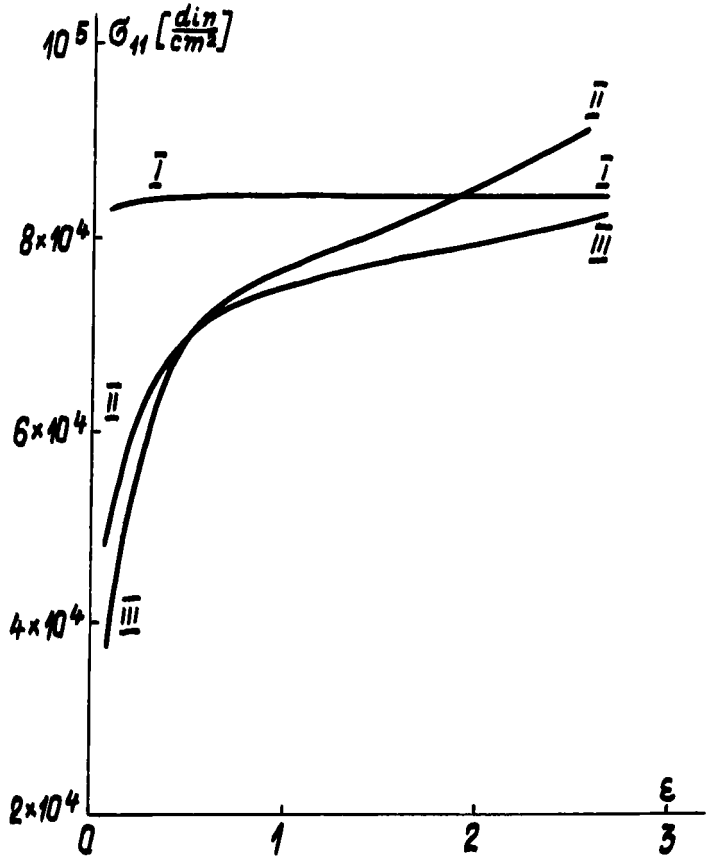

FIGURE 4 Stress *vs.* strain relationship for test samples of different polydispersity u: I, 1.0; II, 12; III, 29, and equal weight-average molecular weight $\bar{M}_w = 10^5$ at elongational strain rate $\dot{\varepsilon} = 0.00137\ \text{sec}^{-1}$.

teristic relaxation time depend on the molecular branching is in no way identical.[18,19]

A Meissner-type apparatus[7,20] was used to stretch two test samples of low-density polyethylene. The test samples had the following molecular values: Test Sample A – $\bar{M}_w = 5.53 \cdot 10^5$, $\langle g \rangle_w = 0.225$, $u = 27$; Test Sample B – $\bar{M}_w = 3.72 \cdot 10^6$, $\langle g \rangle_w = 0.350$, $u = 11$. The difference between weight-average MWs of two test samples was about 30%, and that between coefficients $\langle g \rangle_w$ was about 56% (the long-chain branching node number for the first sample was about two times that of the second test sample). As a result, the predominant effect of the long-chain branching on viscous properties was shown for Test Sample A, even though its molecular weight was higher and its initial viscosity was 7.7 lower than that of Test Sample B (η_0 was $2.90 \cdot 10^5$ p for Test Sample A, and $2.24 \cdot 10^6$ p for Test Sample B).

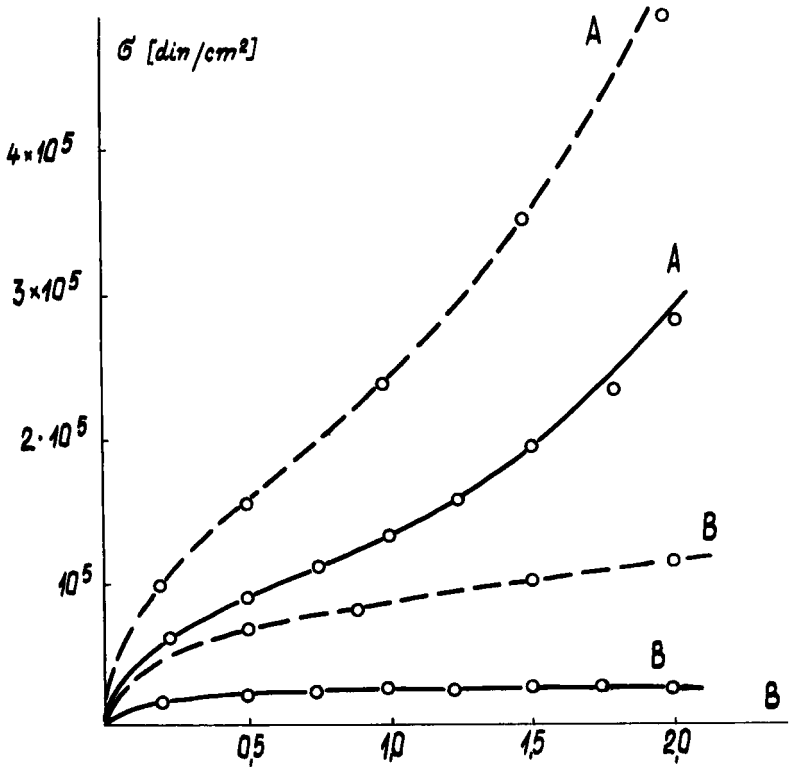

FIGURE 5 Pre-stationary elongational flow of low-density polyethylene at $\dot{\varepsilon} = 0.017$ sec^{-1} (———), $\dot{\varepsilon} = 0.064$ sec^{-1} (– – –). Test Sample A: $\bar{M}_w = 5.58 \cdot 10^5$; $u = 26$; $\langle g \rangle_w = 0.225$. Test Sample B: $\bar{M}_w = 3.72 \cdot 10^5$; $u = 10$; $\langle g \rangle_w = 0.350$. The solid lines are the theoretical curves calculated on the basis of molecular parameters; the dots represent experimental data points.

Figure 5 shows the $\sigma - \varepsilon$ relationship for the two above test samples at two constant strain rate values. The solid lines are the theoretical curves based on calculations of molecular characteristics, and the dots represent the experimental data points. It may be seen that quite different pre-stationary elongational flow curves are obtained for the test samples with different molecular values. For Test Sample B having a much higher Trouton viscosity than Test Sample A (λ is $8.7 \cdot 10^5$ p for Test Sample A, and $6.72 \cdot 10^6$ p for Test Sample B), the axial stresses proved to be several times lower than those for Test Sample B. As stress increase in time for Test Sample B seems to be slowed down due to a much longer relaxation time of this test sample. The Test Sample B relaxation time is longer due to a lower long-chain branching degrees and a larger MWD width.

The — relation does not allow to separately determine the elastic and non-elastic characteristics of the stretched test sample in the pre-stationary flow process.

Elastic properties are normally determined, upon termination of the elongation flow, by the elastic recovery of the test sample released from the grips. Such a determination technique for elastic properties seems to be rather a disputable one, especially when used at higher stretching degrees. Therefore, viscoelasticity characteristics as determined by super-imposing linear deformation on the elongational flow were used to evaluate the viscoelastic properties of a polymer melt under elongational flow conditions.

The experiments were carried out using an extension vibrorheometer where a test sample was stretched by two roller pairs, one pair being involved in oscillatory motion around the equilibrium position in the direction of the elongational axis of the test sample being stretched [7,20] (Figure 6).

The computerized control system[7,20] for the elastically suspended roller pair enables a complex stress-strain ratio for the periodic stress resulting from a periodic displacement of a test sample end to be determined.

If the periodic deformation amplitude is so small that the periodic deformation exerts practically no influence on the stationary flow characteristics, then ratio $\sigma_0 \sin \omega t / [\varepsilon_0 \sin(\omega t + \phi)]$ is arbitrarily taken as the dynamic elongational modulus of the uniaxially extended material.

In the Trouton flow region, i.e. at the deformation rates which lead to the steady elongation flow with the constant viscosity equal to three times the highest shear viscosity, the frequency relations of modulus components $E'(\omega)$ and $E''(\omega)$ are numerically equal to three times the values of shear modulus frequency components $G'(\omega)$ and $G''(\omega)$ measured under linear periodic deformation conditions. The complex elongational modulus components measured by means of periodic deformation are increasing with the elongational stationary deformation rates, this increase for the low-frequency region being more pronounced than that for the high-frequency region. The increase

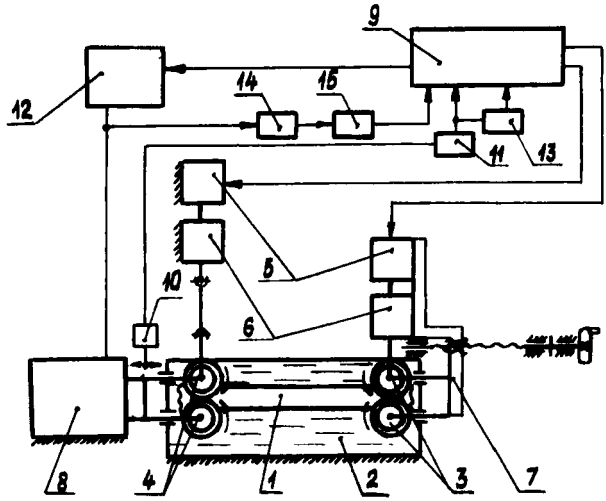

FIGURE 6 Simplified circuit diagram of Model BPP21 Vibrorheometer. 1, test sample; 2, fluid bath; 3, stretching roller pair; 4, oscillatory stretching roller pair; 5, motors; 6, double-reduction gears; 7, original test sample length setting carriage; 8, electrodynamical vibrator; 9, control computer; 10, electromechanical transducers; 11, voltage converter; 13, analog-discrete converter; 12, 14, 15, control circuit elements.

of the real component of the complex modules due to the elongational flow is much greater than that for the imaginary component (Figure 7).

For comparison purposes, the results are given for the linear periodic deformation superposition on the stationary shear flow, made for 8% polyisobutylene solution in cetane. Similarly to the elongational flow case, the stationary shear flow effect is mainly exhibited in the low-frequency end of the $G'(\omega)$ and $G''(\omega)$ relations; however the principal distinction from the elongational complex modulus is that, with the periodic deformation superimposed on the shear flow, the shear modulus component values are smaller than with no stationary flow, while with the periodic deformation superimposed on the elongational flow the elongational modulus component values are greater as compared with the respective values measured under no flow conditions.

The decrease of the real component of the complex shear modulus due to the stationary shear flow is much greater than that of the imaginary component, therefore the loss angle (arc tan G''/G') increases with the stationary strain rates under shear flow conditions. In cases where there is no stationary flow, $E' = 3G'$ and $E'' = 3G''$, therefore arc tan $G''/G' =$ arc tan E''/E'. With the elongational flow setting in, the E' and E'' values become higher, with a more marked increase observed for E'. The resulting loss angle under stationary elongational flow conditions will be smaller than that with no flow present.

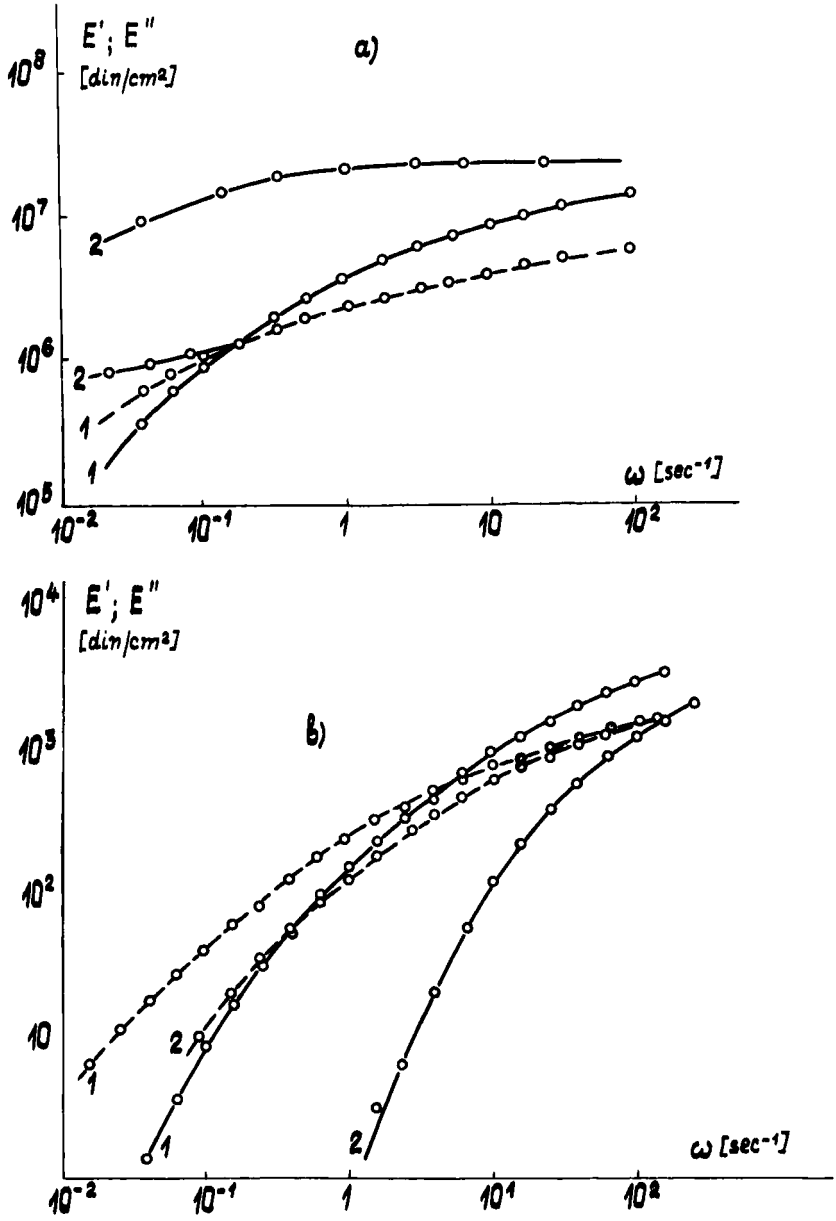

FIGURE 7 (a) Frequency relations of elongational modulus components: (1) under linear periodic deformation of the test sample at rest; (2) same as in (1) with periodic deformation superimposed on stationary elongational flow for polyisobutylene PiB-20. (b) Frequency relations of complex shear modulus: (1) under periodic deformation of the test sample at rest; (2) with periodic deformation superimposed on stationary shear flow for 8% polyisobutylene solution in cetane.

Normally, the largest loss angle values are typical for fluids, while solid bodies are characterized by small loss angle values. The loss angle decreases under elongational flow conditions, and this phenomenon may be regarded as an approach of a fluid material to the solid-like state. The shear flow is characterized by increasing loss angles; thus, the material gets liquefied. Changes in the periodic deformation response of the material occur during the pre-stationary elongational flow. Figure 8 shows changes occurring in longitudinal modulus components $E'(\omega)$ and $E''(\omega)$ during the stationary elongational flow development. It may be seen here that the calculations using Eqs. (7) and (8) in conjunction with the relaxation spectrum provide rather a good representation of the prestationary elongational flow development. The

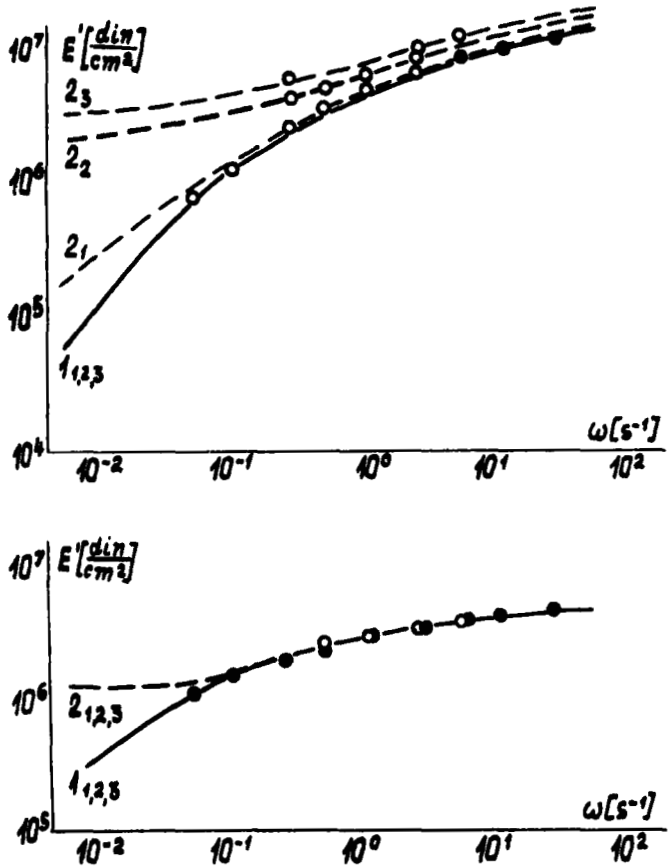

FIGURE 8 E' and E'' frequency relations for polyisobutylene PiB-20 at 19°C under stretching degrees 1_1 and $2_1 - 0.1$; 1_2 and $2_2 - 1.1$; 1_3 and $2_3 - 1.5$. Strain rates $\dot{\varepsilon}$: $1 - 10^{-3}$ sec^{-1}; $2 - 3 \cdot 10^{-1}$ sec^{-1}.

constants which determine the relaxation spectrum were obtained on the basis of the linear periodic shear deformation results.

If, as in Ref. 21, the angular frequency corresponding to the loss angle tan $\delta = 1$ is taken as an arbitrary boundary for the fluid-like state of the substance, then Figure 9 may be used to trace this boundary moving towards lower frequencies as the test sample is extended. The frequency region where the extended material responds like a fluid becomes contracted. Simultaneously, a region resembling a plateau in a similar relation for solid bodies sets in within the low-frequency $G''(\omega)$ region. When studying effects of the molecular structure of a polydisperse polymer on its viscoelastic properties and making use of the above relations for these purposes, it should be borne in mind that a good agreement between theoretical and experimental values is achieved at 10- to 15-fold stretching as dependent on the polymer type. It is for this very reason that effects of the molecular structure on viscoelasticity should be predicted under elongational flow conditions. In addition, consideration should be given to the fact that a comparison is made between different materials of different molecular structures, for which the same stationary flow rate is involved in different ratios to the characteristic relaxation time of the material. Therefore, from the material investigation viewpoints, the molecular effect on viscoelasticity characteristics should be considered at the elongational flow strain rates which are identical with respect to the characteristic relaxation time of each test sample.

From the processing technology viewpoint, of more interest is a comparison between test samples of different molecular structures at the same elongational stationary strain rates. Therefore, both methods will be made use of to assess effects of the molecular structure on the polymer viscoelasticity under elongational flow conditions.

Figures 10 and 11 show frequency relations of the modulus components E' and E'' for two test samples having the same polydispersity indices ($u = 12$) and different weight-average MWs. As may be noted for the low MW test sample under the same elongational flow strain rates, the E' and E'' frequency curves have steeper slopes and the $E'(\omega)$ and $E''(\omega)$ intersection point limiting arbitrarily the fluidity zone length lies in a much higher frequency region. This means that, under the same stretching degrees, the high MW test sample responds as a fluid to the elongational deformation in a narrower frequency (strain rate) region. The higher MW of a test sample, the more pronounced its solid-like response under extension at temperatures corresponding to the fluidity state.

Comparison between $E'(\omega)$ and $E''(\omega)$ of these test samples at the characteristic elongational strain rates ($\varepsilon = 1/\tau_r$) shows the $E'(\omega)$ relations to be different only at low frequencies and in the initial stretching period (at low stretching degrees).

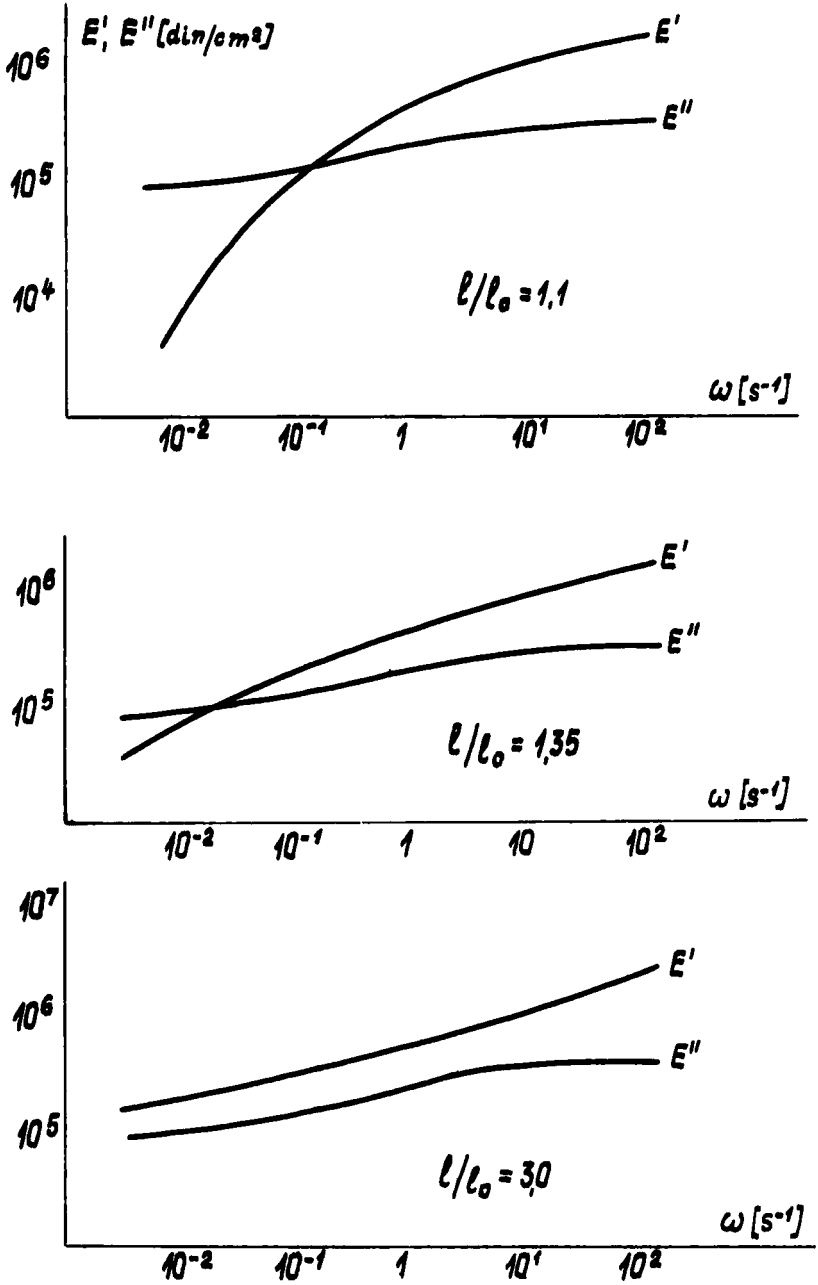

FIGURE 9 Point $E' = E''$ displacement with the test sample extension at frequency relations in the low-frequency region.

Under sufficiently high stretching degrees, the difference between $E'(\omega)$ and $E''(\omega)$ of the two test samples is negligible. The frequency zone of the fluid-like response is somewhat shorter for the low MW test sample.

When comparing the E' and E'' frequency relations of a NMWD ($u = 1$) test sample and a BMWD ($u = 12$) test sample of the same MW under the same strain rates, it may be seen that the curves for the BMWD test have more flat slopes than those for the NMWD test sample (Figure 11). Therefore, at low

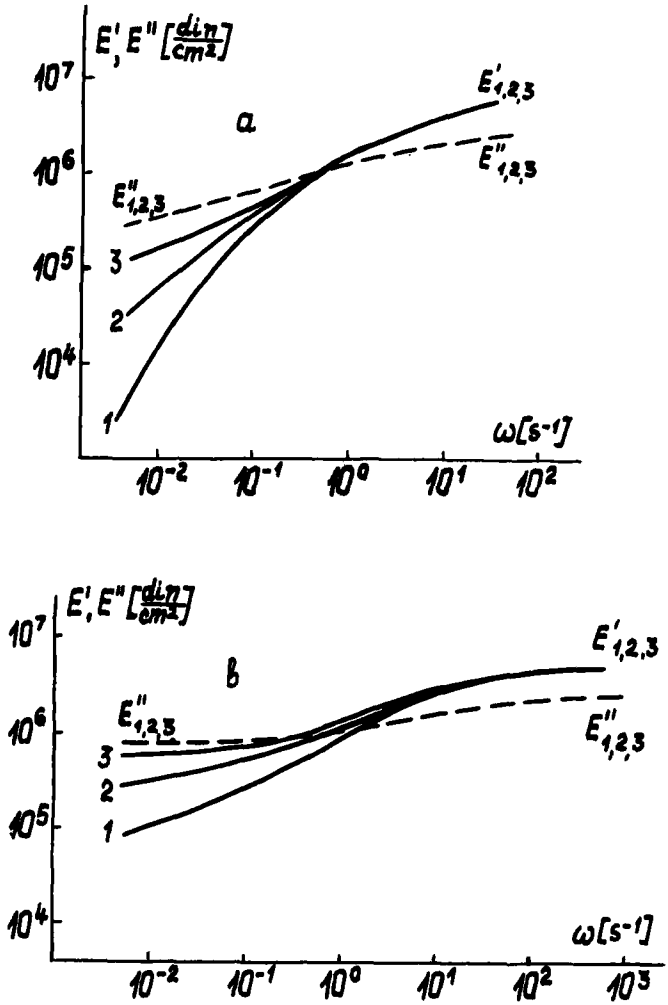

FIGURE 10 E' and E'' frequency relations for equal MWD width test samples with the following $\bar{M}_w$ values: (a), $2.74 \cdot 10^5$; (b), $3.65 \cdot 10^5$. Strain rate for both test samples $\dot{\varepsilon} = 0.038\ \text{sec}^{-1}$; stretching degrees: 1, 0.1, 2, 0.3, 3, 0.5.

deformation frequencies E' is higher for a BMWD polymer, and at high deformation frequencies E' is higher for a NMWD polymer. Under slow stretching conditions, a NMWD material is softer than a BMWD material, and vice versa under fast stretching conditions.

Other molecular values being equal, the characteristic relaxation time of a NMWD polymer is shorter and the characteristic strain rate higher than those for a BMWD polymer.

If the comparison is made at characteristic strain rates, rather flat $E'(\omega)$ and

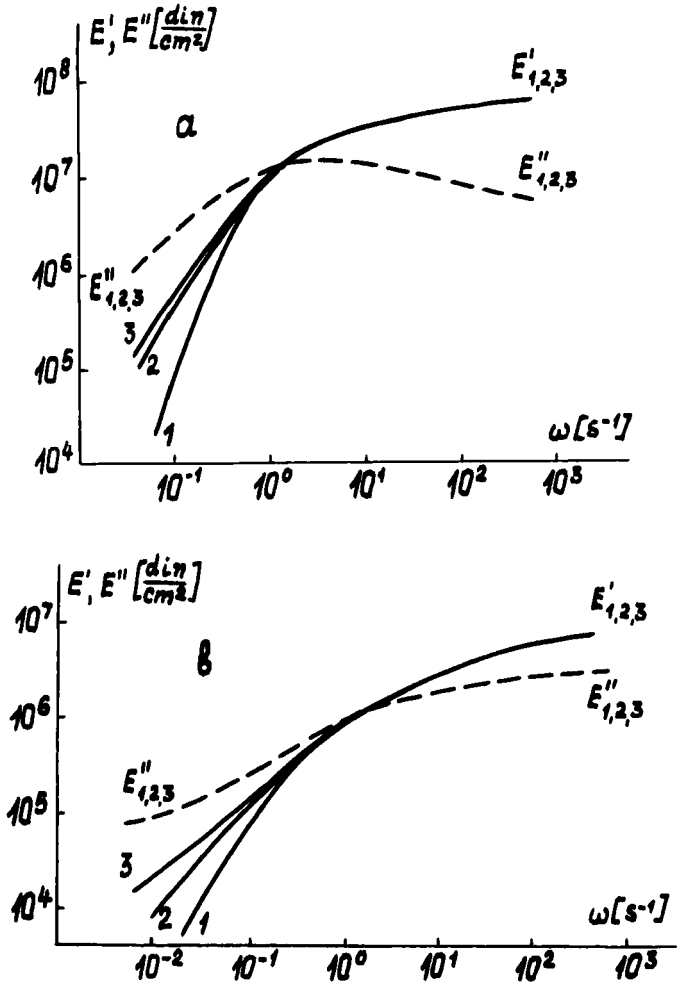

FIGURE 11 $E'(\omega)$ and $E''(\omega)$ relations for test samples with equal $\bar{M}_w = 2.10^5$ and different MW polydispersity: (a) $u = 1.0$; (b) $u = 12$. For strain rates and stretching degrees see Figure 10.

$E''(\omega)$ curves are observed both for NMWD and BMWD polymers (Figure 12). The frequency range of the fluid-like response to periodic deformation seems to be narrower for the BMWD polymer than for the NMWD polymer. As it could be expected, the NMWD polymer is characterized by a higher E' modulus.

At a first glance, rather unexpectedly seems a prolonged and considerable displacement of the fluidity zone boundary as the BMWD polymer is extended, whereas for the NMWD polymer this boundary displacement with the stretching degree is much smaller. Such a behaviour is better understood if E' and E'' are determined following time spans of equal duration rather than under equal stretching degrees. Then it becomes evident that the NMWD polymer is undergoing a more rapid change, as might be expected.

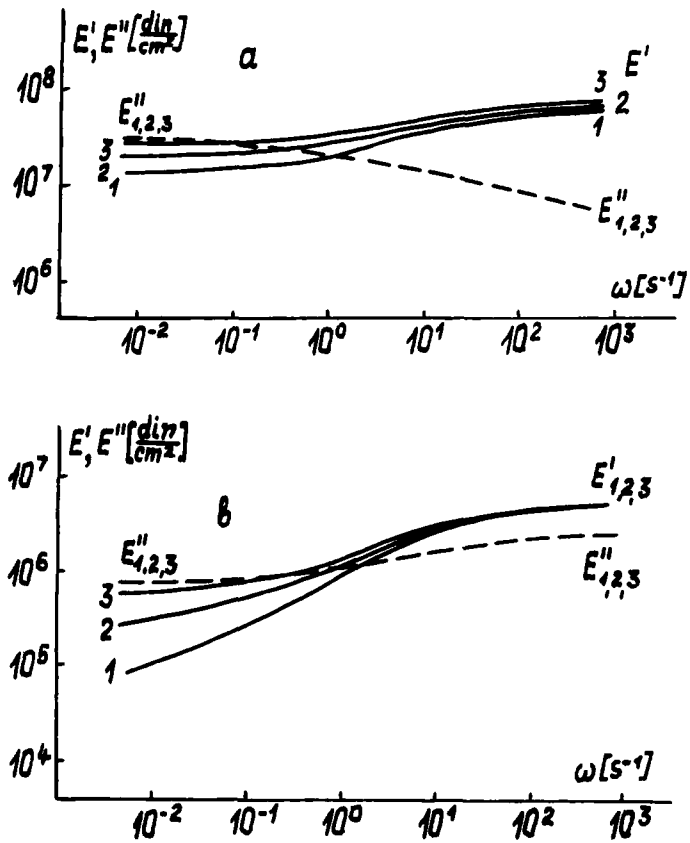

FIGURE 12 $E'(\omega)$ and $E''(\omega)$ relations for the test samples from Figure 11 under stretching conditions at the same strain rate with respect to the characteristic relaxation time: (a) $\dot{\varepsilon} = 0.892$ sec^{-1}; (b) $\dot{\varepsilon} = 0.319$ sec^{-1}.

References

1. A. Malkin, V. Blinova, G. Vinogradov, M. Zaburina, O. Sabsai, V. Shalganova, I. Kirchevskaya and V. Shatalov, *Europ. Polym. J.* **10,** 445 (1974).
2. G. Vinogradov, Macromol. Chem. 8 Plenary and Main Lect. *Int. Symp. Macromol. Helsinki*, 1972 (London 1973), pp. 413–47.
3. G. Vinogradov, in: *Khimiya i Tekhnologiya Visokomolekularnich Soedinenii*, t.5, M., 1974, pp. 130–71.
4. G. Vinogradov and A. Malkin, *Rheologiya Polimerov. M.* (Khimiya, 1977), 440 pp.
5. J. M. Dealy, *Pol. Eng. and Sci.* **6,** 423 (1971).
6. H. M. Lauw and H. Mündstedt, *Rheol. Acta* **15,** 517 (1976).
7. V. Leitlands, *Int. J. Polym. Materials* **8,** 233 (1980).
8. J. A. Spearot and A. B. Metzner, *Trans. Soc. Rheol.* **16,** 495 (1972).
9. P. A. Mendelson, A. Bowles and F. L. Finger, *J. Pol. Sci.* A-2, **8,** 105 (1970).
10. K. Ninomiya and D. Ferry, *J. Colloid Sci.* **18,** 421 (1963).
11. K. Ninomiya, *J. Colloid Sci.* **17,** 759 (1962).
12. J. D. Ferry, *Viscoelastic Properties of Polymers*, 2nd ed. (N.Y., 1970), 671 pp.
13. E. E. Drott and R. A. Mendelson, *J. Pol. Sci.* A-2, **11,** 1361 (1970).
14. W. H. Stockmayer and M. Fihman, *Ann. New York Acad. Sci.* **57,** 334 (1953).
15. B. H. Zimm and W. H. Stockmayer, *J. Chem. Phys.* **17,** 1301 (1949).
16. B. Gross, *Mathematical Structure of the Theories of Viscoelasticity* (Paris, 1953), 74 pp.
17. I. Briedis and L. Faitelson, *Mekhanika Polimerov* **3,** 523 (1975).
18. J. Brauer, I. Briedis, V. Bukhgalter, L. Sulzhenko, L. Faitelson and P. Fidler, *Mekhanika Polimerov* **2,** 283 (1977).
19. I. Briedis and L. Faitelson, *Mekhanika Polimerov* **1,** 120 (1976).
20. V. Leitlands, I. Briedis and P. Adavich, *Ya. Indulevich, Mekhanika Polimerov* **2,** 336 (1976).
21. L. Faitelson, *Int. J. Polym. Mat.* **8,** 207 (1980).